Control of a Drone: Study and Analysis of the Robustness

Kadda M. Zemalache, Lotfi Beji and Hichem Maaref

Abstract:

The work describes an automatically on-line Self-Tunable Fuzzy Inference System (STFIS) of a new configuration of mini-flying called XSF (X4 Stationnary Flyer) drone. A Fuzzy controller based on on-line optimization of a zero order Takagi-Sugeno fuzzy inference system (FIS) by a back propagation like algorithm is successfully applied. It is used to minimize a cost function that is made up of a quadratic error term and a weight decay term that prevents an excessive growth of parameters. Thus, we carried out control for helical trajectories by using the STFIS technique. This permits to prove the effectiveness of the proposed control law. Simulation results and a comparison with a Static Feedback Linearization controller (SFL) are presented and discussed. We studied the robustness of the two used controllers in the presence of disturbances. We presented the case of a engine breakdown as well as a gust of wind and taking into account white noise disturbances.

Keywords: *self-tunable fuzzy inference system, static feedback linearization controller, tracking control, dynamic systems, drone.*

1. Introduction

The past few years have witnessed a rapid growth in the use of fuzzy logic controllers for the control of processes, which are complex and ill defined. Most fuzzy controllers developed till now have been of the rule-based type, where the rules in the controller attempt to model the operator's response to particular process situation.

Recently, the resurgence of interest in the field of artificial neural networks has injected a new driving force into the fuzzy literature. The back-propagation learning rule, which drew little attention till its applications to artificial neural networks was discovered, is actually an universal learning paradigm for any smooth parameterized models, including fuzzy inference systems. As a result, a fuzzy inference system can now not only take linguistic information from human experts, but also adapt itself using numerical data (in-put/output pairs) to achieve better performance. This gives fuzzy inference systems an edge over neural networks, which cannot take linguistic information directly.

In autonomous wheeled robot, many developed learning techniques have arisen in order to generate or to tune fuzzy rules. Most of them are based on the so-called "Neuro-Fuzzy learning algorithms" as proposed by (18; 19; 21; 22; 28; 33). These methods are well for constructing an optimal fuzzy system model which is used to identify the corresponding practical system.

Modeling and controlling aerial vehicles (blimps, mini rotorcraft) are the principal preoccupation of the IBISC-group. Within this optic, which attracted the contest of the DGA-ONERA[1] was the XSF project which consists of a drone with revolving aerofoils (2), (see Fig.1 left). It is equipped with four rotors where two are directionals, what we call in the following X4 Stationary Flyer (XSF).

The XSF is an engine of *68cm* × *68cm* of total size and not exceed *2kg* in mass. It is designed in a cross form and made of carbon fiber. Each tip of the cross has a rotor including an electric brushless motor, a speed controller and a two-blade ducted propeller.The operating principle of the XSF can be presented thus: two rotors turn clockwise, and the two other rotors turn counterclockwise to maintain the total equilibrium in yaw motion. The equilibrium of angular velocities of all rotors done, the Unmanned Aerial Vehicle (UAV) is either in stationary position, or moving vertically. A characteristic of the XSF compared to the existing quadrotors, is the swiveling of the supports of the motors 1 and 3 around the pitching axis thanks to two small servomotors controlling the swiveling angles ξ_1 and ξ_3. This swiveling ensures either the horizontal rectilinear motion or the rotational movement around the yaw axis or a combination of these two movements which gives the turn (see Fig. 1 right). This permits a more stabilized horizontal flight and a suitable cornering. Drone XSF is a flying machine of low dimension able to carry a small payload, in particular a camera, intended to carry out in an autonomous way a reconnaissance mission. In addition to the military applications, this type of machines can also interest the civil field, in particular the search for anybody in buildings in flame, the environmental protection, the natural risk management and the management of the great infrastructures.

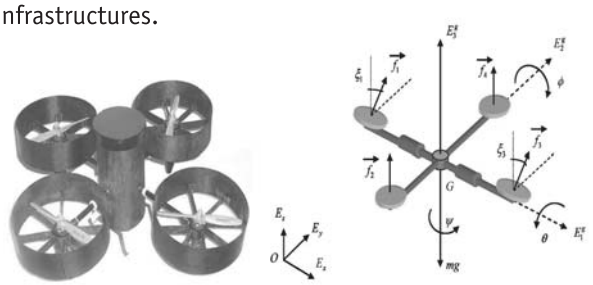

Fig. 1. Conceptual form of the XSF (left), Frames attached to the XSF (right).

1. This work is supported by the mini-flyer competition program organized by the DGA (Direction Générale des Armements) and the ONERA (Office Nationale d'Etude et de Recherche en Aérospatiale), France.

Several recent works were completed for the design and control in pilotless aerial vehicles domain such that Quadrotor (25; 29; 35; 36). Also, related models for controlling the Vertical Take-Off and Landing (VTOL) aircraft are studied by Hauser *et al* (14). A model for the dynamic and configuration stabilization of quasi-stationary flight conditions of a four rotors VTOL, based on Newton formalism, was studied by Hamel *et al* (12) where the dynamic motor effects are incorporating and a bound of perturbing errors was obtained for the coupled system. Castillo *et al* (10) performed autonomous take-off, hovering and landing control of a four rotors by synthesizing a controller using the Lagrangian model based on the Lyapunov analysis.

The stabilization problem of a four rotors rotorcraft is also studied and tested by Castillo (9) where the nested saturation algorithm is used, the input/output linearization procedure (14), in (8) a proportional integral derivative (PID) controller and a linear quadratic (LQ) controller were implemented and proved capable of regulating the system and application of the theory of flat systems by Beji *et al* (4). Mistler et al (27) developed a dynamic model in non linear state space representation and used an exact linearization and non-interacting control for the global system to evaluate translational motion and yaw angle outputs. Mokhtari *et al* (26) proposed an attempt to apply linear H_∞ outer control of helicopter quadrotor with plant uncertainty combined with a robust feedback linearization inner controller. Hanford *et al* (15), presented a simple closed loop equipped with MEMS (Micro-Electro-Mechanical Systems) sensors and PIC based processing unit. Waslander *et al* (34) maked an emphasis on the insufficiency of classical control methods and proposes the integral sliding mode controller associated with reinforcement learning to achieve multi agent control. Tayebi and McGilvray (31) proposed a new quaternion-based feedback control scheme for exponential attitude stabilization of a quadrotor. The proposed controller is based upon the compensation of the Coriolis and gyroscopic torques and the use of a PD^2 feedback structure, where the proportional action is in terms of vector quaternion and the two derivative actions are in terms of airframe angular velocity and vector quaternion velocity. Hoffman *et al* (16; 17), achieved the formation control by sliding mode technique and focused on collision and obstacle avoidance by extracting the state variables with a Kalman filter. Mederreg *et al* (24) developed a non linear controller with observers based on the Backstepping. The robustness of this controller is studied, performances and stability of the suggested controller are analyzed through simulations carried out on the model (kinematics and dynamic equations). In (3), Benzemrane et al adressed the classical problem of speed estimation of an Unmanned Aerial Vehicle when the acceleration, the angles and the angular speeds are available for measurement. A solution has been provided for a class of systems via the tools of adaptive observation theory with promissing results. Bestaoui *et al* (6) addressed the problem of characterizing maneuvers paths on the group of rigid body motions in 3D for a quadrotor. The role of the trajectory generator is to generate a feasible time trajectory for the UAV.

Flight control methods utilizing vision systems are also studied by (32), which exploits the Moiré patterns, and in (1), which utilizes double cameras. Hamel and Mahony (13) proposed a vision based controller which performs visual servo control by positioning a camera onto a fixed target for the hovering of a quadrotor. All the reviewed techniques require the well knowledge of the system dynamic model and parameters. In this paper, a STFIS control strategy is developed based on the systems output measures is implemented. This technique early used for autonomous wheeled robot (22), is adapted and modified for the used with the XSF.

The arrangement of this paper is as follows. The dynamic model of the XSF drone is given in the second section. The developed ideas of control for the XSF by the Self-Tunable Fuzzy Inference System (STFIS) controller is presented and compared with a Static Feedback Linearization controller (SFL) to stabilize the XSF by using the point to point steering stabilization in the third section. Motion planning and simulation results are introduced in the fourth section. The robustness of the proposed controller is then evaluated in the fifth section. Finally, conclusion and future works are given in the last section.

2. Configuration description and modeling

Unlike regular helicopters that have variable pitch angles, an engine has fixed pitch angle rotors and the rotor speeds are controlled to produce the desired lift forces. Basic motions of the XSF can described using the figure 1 (right). Vertical motion is controlled by collectively increasing or decreasing the power for all motors. Lateral motion, in x direction or in y direction, is not achieved by differentially controlling the motors generating a pitching/rolling motion of the airframe that inclines the collective thrust (producing horizontal forces) and leads to lateral accelerations (9; 12). But, two engines of direction are used to permute between the x and y motion.

The XSF is a system consisting of four individual electrical fans attached to a rigid cross frame. We consider a local reference airframe $\Re_G = \{G, E_1^g, E_2^g, E_3^g\}$ at G (mass center) while the inertial frame is denoted by $\Re_O = \{O, E_x, E_y, E_z\}$ such that the vertical direction E_z axis is pointing upwards. Let the vector $X = (x, y, z)$ denotes the G position with respect to $\Re_O$. The rotation of the rigid body is defined by $R_{\phi,\theta,\psi} : \Re_O \rightarrow \Re_G$, where $R_{\phi,\theta,\psi} \in SO$ (3) is an orthogonal rotation matrix which is defined by the An Euler angles, θ (pitch), ϕ (roll) and ψ (yaw), regrouped in $\eta=(\phi, \theta, \psi)$. An Euler angle representation given in Eq. 1 has been chosen (37).

$$R = \begin{pmatrix} C_\psi C_\theta & C_\theta S_\psi & -S_\theta \\ S_\phi C_\psi S_\theta - S_\psi C_\phi & S_\theta S_\psi S_\phi + C_\psi C_\phi & C_\theta S_\phi \\ S_\theta C_\psi S_\phi + S_\psi C_\phi & S_\phi S_\theta S_\psi - C_\psi C_\phi & C_\theta S_\phi \end{pmatrix} \quad (1)$$

Where for example C_θ and S_θ represent $\cos\theta$ and $\sin\theta$ respectively.

2.1. Motion dynamic

We consider the translation motion of $\Re_G$ with respect to $\Re_O$. The position of the mass center *wrt* $\Re_O$ is defined by $\overline{OG} = (x\, y\, z)^T$, its time derivative gives the

velocity *wrt* to $\Re_O$ such that $\frac{d\overline{OG}}{dt} = (\dot{x}\,\dot{y}\,\dot{z})^T$, while the second time derivative permits to get the acceleration $\frac{d^2\overline{OG}}{dt^2} = (\ddot{x}\ddot{y}\ddot{z})^T$ (Fig. 1 (right)).

The model is a simplified one's. The constraints as external perturbation and the gyroscopic torques are neglected. The aim is to control the engine vertically along z axis and horizontally according to x and y axis. The vehicle dynamics, represented on Fig. 1 (right), is modeled by the system of equations 2 (2; 5; 39).

$$\begin{aligned} m\ddot{x} &= S_\psi C_\theta u_2 - S_\theta u_3 \\ m\ddot{y} &= (S_\theta S_\psi S_\phi + C_\psi C_\phi)u_2 + C_\theta S_\phi u_3 \\ m\ddot{z} &= (S_\theta S_\psi S_\phi - C_\psi C_\phi)u_2 + C_\theta S_\psi u_3 - mg \end{aligned} \quad (2)$$

m is the total mass of the vehicle. The vector u_2 and u_3 combines the principal non conservative forces applied to the engine airframe including forces generated by the motors and drag terms. Drag forces and gyroscopic due to motors effects will be not considered in this work. The lift (collective) force u_3 and the direction input u_2 are such that

$$\begin{pmatrix} 0 \\ u_2 \\ u_3 \end{pmatrix} = f_1\acute{e}_1 + f_2 e_2 + f_3\acute{e}_3 + f_4 e_4 \quad (3)$$

with $f_i = K_T\omega_i^2$ where $K_T = 10^{-5}N.s^2$ and ω_i is the angular speed resulting of motor i. Let

$$\acute{e}_1 = \begin{pmatrix} 0 \\ S_{\xi_1} \\ C_{\xi_1} \end{pmatrix}_{\Re_G}; \acute{e}_3 = \begin{pmatrix} 0 \\ S_{\xi_3} \\ C_{\xi_3} \end{pmatrix}_{\Re_G}; e_2 = e_4 = \begin{pmatrix} 0 \\ 0 \\ 1 \end{pmatrix}_{\Re_G} \quad (4)$$

Then we deduce:

$$\begin{aligned} u_2 &= f_1 S_{\xi 1} + f_3 S_{\xi 3} \\ u_3 &= f_1 C_{\xi 1} + f_3 C_{\xi 3} + f_2 + f_4 \end{aligned} \quad (5)$$

ξ_1 and ξ_3 are the two internal degree of freedom of rotors 1 and 3, respectively. These variables are controlled by dc-motors and bounded $-20° \leq \xi_1, \xi_3 \leq +20°$. e_2 and e_4 are the unit vectors along E_3^g which imply that rotors 2 and 3 are identical of that of a classical quadrotor (37; 38).

2.2. Rotational motion

The rotational motion of the XSF will be defined *wrt* to the local frame but expressed in the inertial frame.

Where the inertia elements I_{xx}, I_{yy} and I_{zz} are of the inertia matrix I_G expressed in G, then $I_G = diag\,(I_{xx}, I_{yy}, I_{zz})$.

$$\begin{aligned} \ddot{\theta} &= \tfrac{1}{I_{xx}C_\phi}(\tau_\theta + I_{xx}S_\phi\dot{\phi}\dot{\theta}) \\ \ddot{\phi} &= \tfrac{1}{I_{yy}C_\theta C_\phi}(\tau_\phi + I_{yy}S_\phi C_\theta\dot{\phi}^2 + I_{yy}S_\theta C_\phi\dot{\theta}\dot{\phi}) \\ \ddot{\psi} &= \tfrac{\tau_\psi}{I_{zz}} \end{aligned} \quad (6)$$

With the three inputs in torque

$$\begin{aligned} \tau_\theta &= l\,(f_2 - f_4) \\ \tau_\phi &= l\,(f_1 C_{\xi_1} - f_3 C_{\xi_3}) \\ \tau_\psi &= l\,(f_1 S_{\xi_1} - f_3 S_{\xi_3}) + \tfrac{K_M}{K_T}\,(f_1 C_{\xi_1} - f_3 C_{\xi_3} + f_4 - f_2) \end{aligned} \quad (7)$$

where l is the distance from G to the rotor i and $K_M = 9.10^{-6}N.m.s^2$. The equality from Eq. 6 is ensured, meaning that:

$$\ddot{\eta} = \Pi_G(\eta)^{-1}\left[\tau - \dot{\Pi}_G(\eta)\,\dot{\eta}\right] \quad (8)$$

With $\tau = (\tau_\theta, \tau_\phi, \tau_\psi)^T$ as an auxiliary inputs.
And

$$\Pi_G(\eta) = \begin{pmatrix} I_{xx}C_\phi & 0 & 0 \\ 0 & I_{yy}C_\phi C_\theta & 0 \\ 0 & 0 & I_{zz} \end{pmatrix} \quad (9)$$

As a first step, the model given above can be input/output linearized by the following decoupling feedback laws

$$\begin{aligned} \tau_\theta &= -I_{xx}S_\phi\dot{\phi}\dot{\theta} + I_{xx}C_\phi\tilde{\tau}_\theta \\ \tau_\phi &= -I_{yy}S_\phi C_\theta\dot{\phi}^2 - I_{yy}S_\theta C_\phi\dot{\theta}\dot{\phi} + I_{yy}C_\theta C_\phi\tilde{\tau}_\phi \\ \tau_\psi &= I_{zz}\tilde{\tau}_\psi \end{aligned} \quad (10)$$

and the decoupled dynamic model of rotation can be written as

$$\ddot{\eta} = \tilde{\tau} \quad (11)$$

with $\tilde{\tau} = (\tilde{\tau}_\theta\tilde{\tau}_\phi\tilde{\tau}_\psi)^T$

Using the system of equations Eq. 2 and Eq. 11, the dynamic of the system is defined by

$$\begin{aligned} m\ddot{x} &= S_\psi C_\theta u_2 - S_\theta u_3 \\ m\ddot{y} &= (S_\theta S_\psi S_\phi + C_\psi C_\phi)\,u_2 + C_\theta S_\phi u_3 \\ m\ddot{z} &= (S_\theta S_\psi C_\phi - C_\psi S_\phi)\,u_2 + C_\theta C_\phi u_3 - mg \\ \ddot{\theta} &= \tilde{\tau}_\theta \\ \ddot{\phi} &= \tilde{\tau}_\phi \\ \ddot{\psi} &= \tilde{\tau}_\psi \end{aligned} \quad (12)$$

The rotational part can be easily linearized with static feedback control laws. Then, we get:

$$\begin{aligned} \ddot{\theta} &= u_4 \\ \ddot{\phi} &= u_5 \\ \ddot{\psi} &= u_6 \end{aligned} \quad (13)$$

with:

$$\begin{aligned} u_4 &= \tfrac{1}{I_{xx}C_\phi}(\tau_\theta + I_{xx}S_\phi\dot{\phi}\dot{\theta}) \\ u_5 &= \tfrac{1}{I_{yy}C_\theta C_\phi}(\tau_\phi + I_{yy}S_\phi C_\theta\dot{\phi}^2 + I_{yy}S_\theta C_\phi\dot{\theta}\dot{\phi}) \\ u_6 &= \tfrac{1}{I_{zz}}\tau_\psi \end{aligned} \quad (14)$$

Remark As shown in Eq. 2, the equivalent system of control-inputs presents five inputs $U = (u_2, u_3, u_4, u_5, u_6)$, while the rotor force-inputs are of six order $F = (f_1, f_2, f_3, f_4, \xi_1, \xi_3)$. Then the transformation $U \to F$ is not a diffeomorphism.

3. Advanced Strategies of control

The aim in this section is to make comparison between model based approaches and experts analysis involving fuzzy systems. Classical model based techniques such us the *static feedback linearization* and *backstepping* techniques have been investigated and used for stabilization with motion planning (5; 39; 23).

3.1. Static Feedback Linearization controller

3.1.1. Control input for z - y motions

We propose to control the *y*/*z* motion through the input u_2/u_3. So, we have the following proposition.

Proposition Consider $(\psi, \theta) \in]-\pi/2, \pi/2[$, with the static feedback laws.

$$\begin{aligned} u_2 &= m\nu_y C_\phi C_\psi^{-1} - m(\nu_z + g) S_\phi C_\psi^{-1} \\ u_3 &= m\nu_y (S_\phi C_\theta^{-1} - C_\phi t g_\psi t g_\theta) + \\ &\quad + m(\nu_z + g)(C_\phi C_\theta^{-1} + S_\phi t g_\psi t g_\theta) \end{aligned} \tag{15}$$

The dynamic of y and z are linearly decoupled and exponentially-asymptotically stable with the appropriate choice of the gain controller parameters. ν_y and ν_z are detailed in the following.

We can regroup the two dynamics as:

$$\begin{pmatrix} \ddot{y} \\ \ddot{z} \end{pmatrix} = \frac{1}{m} \begin{pmatrix} S_\theta S_\psi S_\phi + C_\psi C_\phi & C_\theta S_\phi \\ S_\theta S_\psi C_\phi - C_\psi S_\phi & C_\theta C_\phi \end{pmatrix} \begin{pmatrix} u_2 \\ u_3 \end{pmatrix} - \begin{pmatrix} 0 \\ g \end{pmatrix} \tag{16}$$

For the given conditions in ψ and θ the (2×2) matrix in Eq. 16 is invertible. Then a nonlinear decoupling feedback permits to write the following decoupled linear dynamics.

$$\begin{aligned} \ddot{y} &= \nu_y \\ \ddot{z} &= \nu_z \end{aligned} \tag{17}$$

Then we can deduce from Eq. 17 the linear controller:

$$\begin{aligned} \nu_y &= \ddot{y}_r - k_y^1(\dot{y} - \dot{y}_r) - k_y^2(y - y_r) \\ \nu_z &= \ddot{z}_r - k_z^1(\dot{z} - \dot{z}_r) - k_z^2(z - z_r) \end{aligned} \tag{18}$$

with the k_y^i, k_z^i are the coefficients of a Hurwitz polynomial. Our second interest is the (x,z) dynamics which can be also decoupled by a static feedback law.

3.1.2. Input u2 for the motion along x

The aim here is to stabilize the dynamics of x with the control input u_2. While we keep the input u_3 for the altitude z stabilization.

Proposition with the new inputs

$$\begin{aligned} u_2 &= (S_\psi C_\phi - S_\theta C_\psi S_\phi)^{-1}(m\nu_x C_\phi C_\theta + m(\nu_z + g) S_\theta) \\ u_3 &= (S_\psi C_\phi - S_\theta C_\psi S_\phi)^{-1}(-m\nu_x (S_\psi S_\theta C_\phi - C_\psi S_\phi) + \\ &\quad + m(\nu_z + g) S_\psi C_\theta) \end{aligned} \tag{19}$$

The dynamic of x and z are decoupled and exponentially stable. ν_x and ν_z can be deduced as in Eq. 20 (5).

$$\begin{aligned} \ddot{x} &= \nu_x \\ \ddot{z} &= \nu_z \end{aligned} \tag{20}$$

Remark To switch between the two controllers Eq. 15 and Eq. 19 continuity is recommended allowing the avoidance of the peak phenomenon. This can be asserted if we impose some constraints to the reference trajectories. In order to ensure this, we take $u_2(\psi = 0) = u_2(\psi = \pi/2) = 0$ with $\phi = \theta = 0$. For $\psi = 0$ one uses (15) and for $\psi = \pi/2$ expression Eq. 19 is considered. As soon as we get $u_3(\psi = 0) = u_3(\psi = \pi/2) = mg$ taking $\phi = \theta = 0$.

3.2. Self-Tunable Fuzzy Inference System

The formal analogy between a fuzzy inference system and a multilayer neural network associated with optimization algorithms is used from the retro-propagation gradient algorithm have winded up in what is called a STFIS Network.

3.2.1. Presentation of STFIS

A Sugeno type fuzzy system is determined in three stages (30):

1. Given an input x a membership degree μ is obtained from the antecedent part of rules.
2. A truth value degree α_i is obtained, associated to the premises of each rule R_i:
   IF x_1 is X_1 AND IF x_2 is X_2 THEN u IS w_i.
3. An aggregation stage to take in to account all rules by $u = \sum_{i=1}^{r} \alpha_i w_i / \sum_{i=1}^{r} \alpha_i$ permit to obtain a crisp value u.

These operations can be traduced by the layer structure shown in Fig. 2. Each layer, connected with others by adjustable parameters, having a specific function.

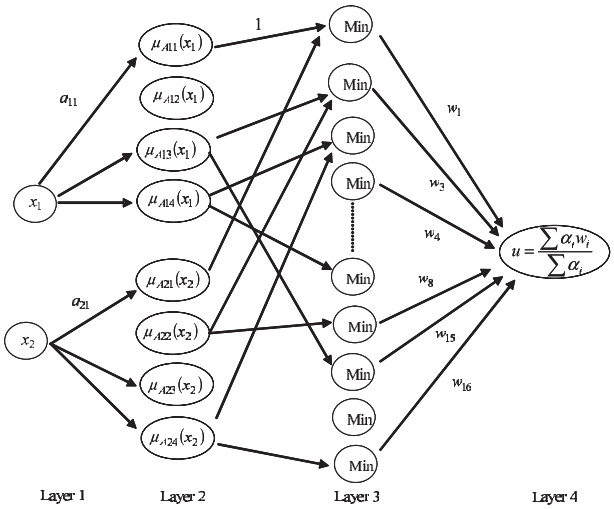

Fig. 2. Self-Tunable Fuzz Inference System.

3.2.2. Architecture and Learning Algorithm Architecture

In this work, we propose to generate the fuzzy control rules by an optimization method, which is done entirely on-line. Jordan (20) proposes the *distal control* method, which is used under the name of JEAN (Jordan method Extended for Adaptive Neurocontrol). This architecture (Fig. 3 a) needs the used of two STFIS networks:

1. A first networks to identify the drone (Model).
2. A second networks to control the drone (Controller).

For the control of the XSF, we have used the architecture known as the "mini-JEAN" as illustrated in the Fig. 3 (b). This architecture not require an emulator net-work. It uses only one network as a controller, the learning of which is done directly by the backpropagation of the output error.

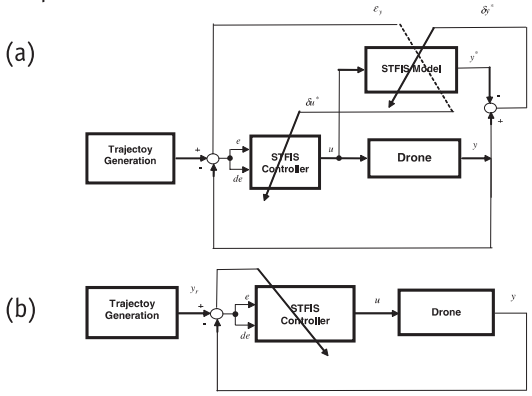

Fig. 3. JEAN Learning Architecture (a), Control architecture mini-JEAN (b).

Compared to the architecture JEAN, some equivalent performances are obtained for the mean error in generalization. On the other hand, the computing time favors clearly mini-JEAN. Optimization of adjustable parameter is accomplished with a version of the classic gradient retro-propagation algorithm adapted to net structure of Fig. 3 (right). The aim is to minimise cost function E:

$$E = \frac{1}{2}\epsilon^2 \tag{21}$$

where ∈ is the difference between set point and process output. The basic equations of the algorithm are:

$$w_{ij}^n(t) = w_{ij}^n(t-1) + \Delta w_{ij}^n(t) \tag{22}$$

$$\Delta w_{ij}^n(t) = -\eta\delta_i^n\alpha_j^{n-1} + b\Delta w_{ij}^n(t-1) \tag{23}$$

Where:
$w_{ij}^n(t)$: i^{th} parameter between i of layer n and j^{st} unit of layer n-1.
η : learning gain.
t : training iteration.
b : moment parameter.
δ_i^n : error term (i^{th} neurone of layer n).
α_j^{n-1} : output of j^{th} unit of layer n-1.

The quality of solution obtained using this algorithm depends on input learning signals, algorithm control parameters and learning duration (number of iterations).

3.2.3. Algorithm Modification Weight Regression

The procedure is entirely done on-line on the engine. The table of rules (weights w_i) can be initially empty or filled with an a priori knowledge. The engine acquires by its systems output measures, calculates the error to the back-propagated, updates the triggered rules on-line. The weights of the table of decision are then adjusted locally and progressively. The cost function is given by:

$$J = E + \lambda\sum w_i^2 \tag{24}$$

where E is the classic quadratic error, w are the parameters (weights) to optimize parameters and λ is a constant that controls the growth of parameters. The second term in J is known as *weight decay* and used usually in the context of classification problems. This technique has been analyzed in the framework of learning theory and it was shown that is a very simple manner to implement a *regularization* method in a neural network in order to optimize the compromise between the learning error and the generalization error (7; 11). Thanks to the classic back-propagation algorithm, the parameters are modify as:

$$w(t+1) = w(t) + \eta(\frac{-\partial J}{\partial w}) \tag{25}$$

This algorithm easily includes the effect of the second term of the cost function J and by taking $\beta = 2\lambda\eta$ (regression coefficient) we obtain:

$$w(t+1) = w(t) + \eta(\frac{-\partial E}{\partial w}) - \beta w(t) \tag{26}$$

Since a fuzzy inference system is concerned, we adapt this formula by multiplying β by the firing term of the rule, namely $\alpha_i/\sum\alpha_i$. α_i is the truth value of the premise part of the triggered rule.

If we limit the optimization only on the conclusions parameters w_{1j}^4. Then, we get

$$\Delta w_{1j}^4(t) = -\eta\delta_1^4\alpha_j^3 + b\Delta w_{1j}^4(t-1) - \tag{27}$$
$$-\alpha_j^3 2\eta\lambda w_{1j}^4(t-1)/\sum_k \alpha_k^3$$

with

$$\delta_1^4 = y_1 - y/\sum_j \alpha_j^3 \tag{28}$$

Where:
y_1 : effective output value.
y : desired output.

4. Motion planning and simulation results

The XSF is tested in simulation in order to validate some motion planning algorithm considering the proposed STFIS control laws. We have considered a total mass equal to $m = 2kg$. The technical characteristics of this flying vehicle were presented in (2). We solve the tracking control problem using the point to point steering stabilization (see (5; 37) for more details).

A Fuzzy controller based on an on-line optimization of a zero order Takagi-Sugeno fuzzy inference system is successfully applied. It is used to minimize a cost func-

tion that is made up of a quadratic error term and a weight decay term that prevents an excessive growth of parameters of the consequent part. The main idea is to generate the conclusion parts (so-called weight) of the rules automatically thanks to an optimization technique. The used method is based on a back-propagation algorithm where the parameters values are free to vary during the optimization process. Starting with a preinitialized rules table, when XSF begins to fly, it performs the acquisition of the distances (observations), calculates the cost function to back-propagation, updates the triggered rules in real time, begins to move and so on. The weights wi are then adjusted locally and progressively. The shape of the used membership functions is triangular and fixed in order to extract and represent the knowledge from the final results easily. To deduce the truth value, we use the MIN operator for the composition of the input variables. For the control of the XSF, we use the architecture known as "mini-JEAN". The universes of discourse are normalized and shared in five fuzzy subsets for all displacement.

The linguistic labels are defined as follows: **NB**: *Negative Big*, **NS**: *Negative Small*, **Z**: *approximately Zero*, **PS**: *Positive Small* and **PB**: *Positive Big*. For exmaple, the results of the simulation are reported in the table 1 for *z* displacement for helical trajectory.

Table 1. Learning weights for z displacement.

de \ e	NB	NS	Z	PS	PB
PB	29.71	30.19	9.31	3.84	1.15
PS	29.69	29.31	10.74	9.77	1.96
Z	39.56	28.85	19.03	11.42	1.8
NS	38.36	37.80	24.01	8.48	9.6
NB	39.76	39.98	28.51	8.15	9.2

Table 2. Learning linguistic table.

de \ e	NB	NS	Z	PS	PB
PB	B	B	W	VW	VW
PS	B	B	W	W*	VW
Z	VB	B	M	W	VW
NS	VB	VB	M*	W	W
NB	VB	VB	B	W	W

The outputs linguistic labels could be interpreteted as follows (Fig. 4): **VW**: [1, 4] *Very Weak*, **W**: [8, 12] *Weak*, **M**: [19, 24] *Medium*, **B**: [28, 31] *Big* and **VB**: [37, 40] *Very Big*.

Table 3. Expertise linguistic table.

de \ e	NB	NS	Z	PS	PB
PB	B	B	W	VW	VW
PS	B	B	W	VW	VW
Z	VB	B	M	W	VW
NS	VB	VB	B	W	W
NB	VB	VB	B	W	W

The table 2, illustrates the linguistic translation of the table obtained by on-line optimization for the *z* displacement for helical trajectory (Table 1). By comparing the table proposed by learning and by human expertise (table 2 and table 3), we can observe that the two sets of linguistic rules are quite close. Two cases (noted with*) are different and they differ from only one linguistic concept (M instead B and W instead VW). So, we can claim that the extracted rules are quite logical and coherent. On the other hand, the main advantage of the described technique is the optimization of the controller with respect to the actual characteristics of the engine.

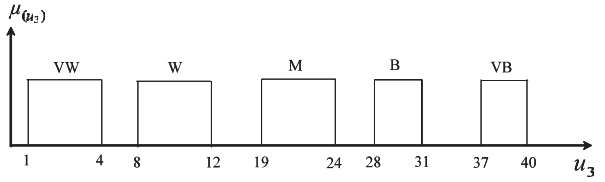

Fig. 4. Representation of the linguistic translation of the controller u_3 for z displacement.

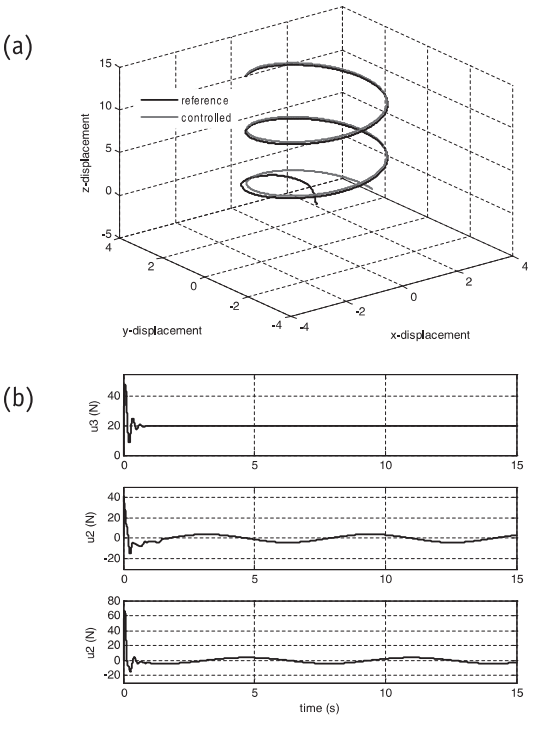

Fig. 5. Realization of a helical trajectory (a), Inputs u_3 and u_2 for the realization of a helical (b).

According to the figure 5 which represents the realization of a helical trajectory (a) and its inputs (b) that our controller ensures the trajectory continuation. In the same figure, it shows the controlled positions *zxy* using STFIS controller where u_3 and u_2, denote the command signals for z, x or y directions respectively. Note that the input $u_3 = mg$ at the equilibrium state is verified.

5. Controllers robustness

5.1. Disturbances with actuator/sensor failures and wind influence

The robustness of the developed controllers are evaluated regarding external disturbances and performance degradations in the case of actuator/sensor failures and wind influence. In the case of the XSF, a resistance or a drag force is opposed to its movement in flight. The work produced by this force involves an additional energy consumption at the actuators levels which limits its maneuvering capacities in flight. This force can be expressed as follow:

$$F_i = \frac{1}{2} C_x \rho A V_i^2 \qquad (29)$$

where F_i [N] is the drag force following the i axis, V_i $[m/s]$ is the drone velocity, A $[m^2]$ is the coss-sectional area perpendicular to the force flow and ρ $[Kg/m^3]$ is the body density. The equation 29 induced a drag coefficient C_x which is a dimensionless quantity that describes a characteristic amount of aerodynamic drag depending on the XSF structure and which is experimently determined by windtunnel tests. This coefficient is equal to 0.5 for the x and y directions and 0.08 for the z displacement. The surface characteristic A of the XSF drone is equal to $A = 0.031\ m^2$ and it density is considered equal to $\rho = 1.22 Kg/m^3$.

(a)

(b)

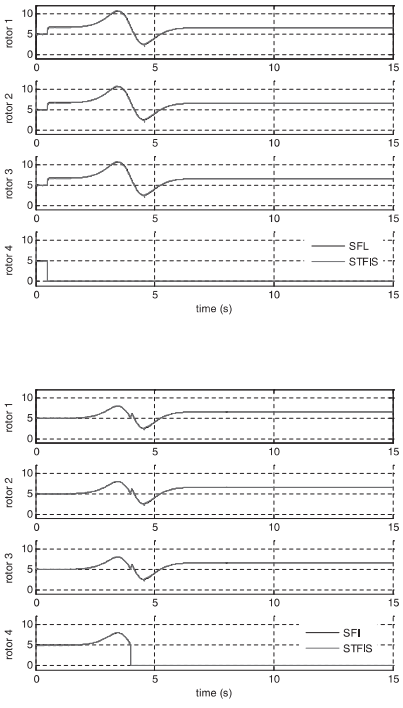

Fig. 6. XSF Forces in the case of motor 4 failure at t = 0.5 s (a) and t = 4 s (b).

(a)

(b)

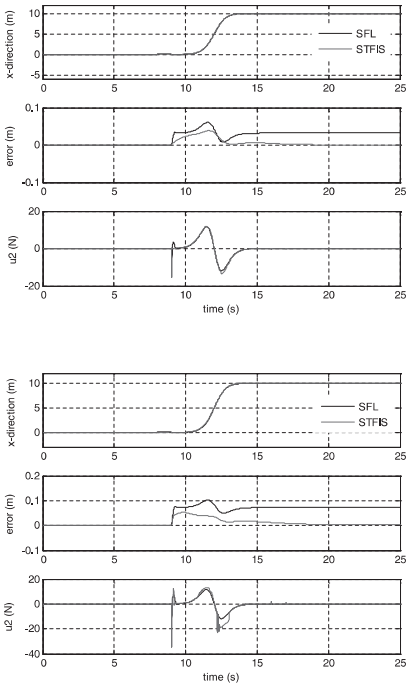

Fig. 7. Wind influence with a drag force of 1.4N (a) and 2.1N (b) for the x direction.

The Fig. 6 illustrate the simulation results in the case of actuator 4 failure after takeoff at the instant $t_1 = 0.5\,s$ and $t_2 = 4\ s$ in the z direction. To maintain its equilibrium, the three remain actuators share the drone load compensation and which practically results in an equitable distribution of the developed forces $(F_1 + F_2 + F_3 = mg$ at steady state). The STFIS and the SFL controllers behaves in the same way.

The Fig. 7 present the simulation results in the case of a drag force of $F_{dg} = 1.4N$ and of $F_{dg} = 2.1N$ according to the x displacement. The STFIS controller exhibits chattering signal problems in the transition phase while the SFL controller presents static errors that varies proportionally with the drag force amplitude F_{dg}. The same observations are found according to the two directions y and z.

5.2. White noise disturbances

The robustness study was realized in simulations taking into account disturbances with a white noise. We considered two cases, in the first one, the noise power is equal to 0.5 and 2 decibel in the second case for both SFL and STFIS controller along the z direction.

The Fig. 8 illustrates simulation results for vertical flight with the application of a white noise at the instant t = 8 s for SFL controller.

In the same way, Fig.9 shows the same tests with STFIS controller. It is noticed that the error is significantly low.

To see the behavior of two controllers according to noise measurement, the figure Fig.10, shows the allure vertical flight for both controller. It is noticed that the STFIS controller gives good results compared to the SFL controller.

(a)

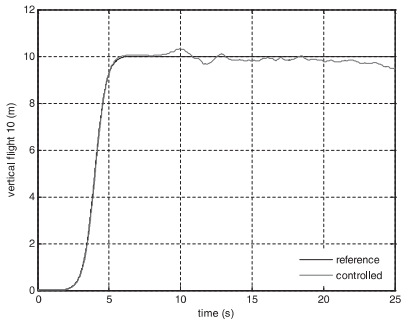

(b)

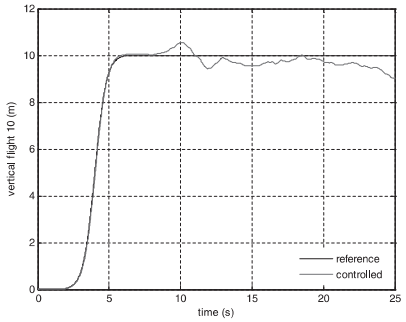

Fig. 8. Vertical flight with white noise and noise power 0.5 dB (a) and 2 dB (b) for SFL controller.

(a)

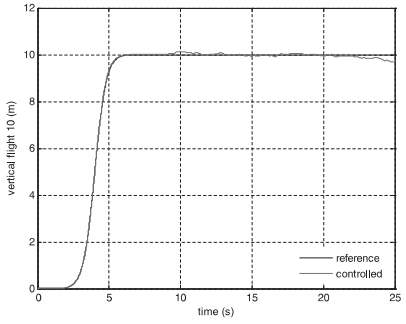

(b)

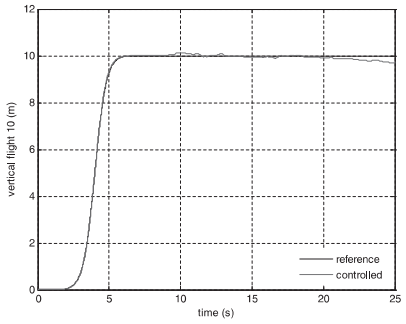

Fig. 9. Vertical flight with white noise and noise power 0.5 dB (a) and 2 dB (b) for STFIS controller.

(a)

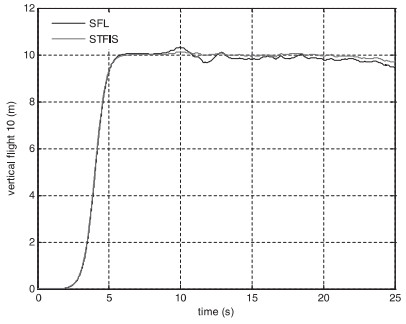

(b)

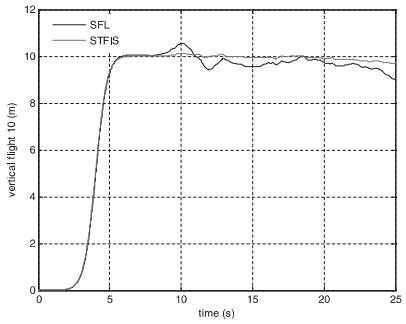

Fig. 10. Vertical flight with noise power 0.5 dB (a) and 2 dB (b) for both controller.

6. Conclusions

In this paper, we studied a new configuration of flyer engine called XSF. We considered in this work the stabilizing/tracking control problem for the three decoupled displacements of a XSF and we performed experiments on helical trajectories. We have presented and implemented an optimization technique allowing an on-line adjustment of the fuzzy controller parameters. The descent gradient algorithm, with its capacities to adapt to unknown situations by the means of its faculties of optimization, and the fuzzy logic, with its capacities of empirical knowledge modelling, are combined to control a new configuration of flyer engine. Indeed, we have obtained an on-line optimized Takagi-Sugeno type SIF of zero order. This method is simple, economical and safe since it is done on a mini-flying robots. It leads to very quick and efficient optimization technique. A comparison between the STFIS set rules and that deduced by human expertise, shows the validity of the proposed technique. An analysis of the STFIS (which not require the good knowledge of the model) and the SFL (requires the well knowledge of the system model and parameters) controllers and their robustness regarding disturbances, shows the advantages and the disadvantages of these two techniques and the influence of white noise disturbances for z direction only. Future works will essentially investigate the real time implementation of the STFIS and the based-model control techniques.

AUTHORS

K. M. Zemalache, L. Beji and H. Maaref - IBISC Laboratory, CNRS- FRE 28 73, Université d 'Evry Val d 'Essonne 40, rue du Pelvoux, 91020, Evry Cedex, France. E-mails: kadda.zemalache@ibisc.univ-evry.fr, lotfi.beji@ibisc.univ-evry.fr, hichem.maaref@ibisc. univ-evry.fr.

References

[1] E. Altug, J. P. Ostrowski and C. Taylor, “Quadrotor control using dual visual feed-back”. In: *Proceeding of the IEEE International Conference on Robotics and Automation*, Taipei, Taiwan, September 2003, pp. 4294-4299.

[2] N. Azouz and Y. Bestaoui, “Modelling and simulation ofa mini quad-rotor helicopter”. In: *Proceeding of DTM-2005, ASME Design Theory and Methodology Conferences*, Long Beach, California, USA, September 2005.

[3] K. Benzemrane, G. L. Santosuosso and G. Damm, "UnmannedAerial Vehicle Speed Estimation Via Nonlinear Adaptive Observers", *American Control Conference*, New York City, USA, 11th-13th July, 2007.

[4] L. Beji and A. Abichou, "Streamlined rotors mini rotorcraft: Trajectory generation and tracking", *International Journal of Automation and Systems*, vol. 3, no. 1, 2005, pp. 87-99.

[5] L. Beji, A. Abichou and K. M. Zemalache, "Smooth control ofanX4 bidirectional rotors flying robots", *Fifth International Workshop on Robot Motion and Control*, Dymaczewo, Poland, June 2005.

[6] Y. Bestaoui and R. Slim, "Maneuvers for a Quad-Rotor Autonomous Helicopter", *AIAA*, Rohnert Park, California, 7-10 May 2007.

[7] C. M. Bishop, "Regularization and complexity control in feedforward neural networks". In: Proc. IEEE Int. Conf. on Neural Networks, Paris, vol. 1, 1995, pp. 141-148.

[8] S. Bouabdallah, A. Noth and R. Siegwart, "PID vs LQ control techniques applied to an indoor micro quadrotor". In: *Proceeding of the IEEE, International Conference on Robotics and Automation*, Barcelona, Spain, April 2005, pp. 2259-2264.

[9] P. Castillo, A. Dzul and R. Lozano, "Real-time stabilization and tracking of a four rotor mini-rotorcraft", *IEEE Transactions on Control Systems Technology*, vol. 12, no. 4, July 2004, pp. 510-516.

[10] P. Castillo, R. Lozano and A. Dzul, "Stabilization ofa mini-rotorcraft having four rotors", *Proceedings of IEEE/RSJ International Conference on Intelligent Robots and Systems*, Sendai, Japan, 2004, pp. 2693-2698.

[11] M.Y. Chow, "An analysis of weight decay as a methodology of reducing three-layer feedforward artificial neural network for classification problems", *ICNN'94, Proc. IEEE Int. Conf. on Neural Networks*, Orlando, vol. 1, 1995, pp. 600-605.

[12] T. Hamel, R. Mahony, R. Lozano and J. P. Ostrowski, "Dynamic modelling and configuration stabilization for an X4-flyer", *IFAC 15th World Congress on Automatic Control*, Barcelona, Spain, 2002.

[13] T. Hamel and R. Mahony, "Pure 2D Visual Servo control for a class of under-actuated dynamic systems". In: *Proceeding of the 2002 IEEE International Conference on Robotics and Automation*, New Orleans, LA, 2004, pp. 2229-2235.

[14] J. Hauser, S. Sastry and G. Meyer, "Nonlinear control design for slightly non-minimum phase systems: application to V/STOL aircraft", *Automatica*, vol. 28, no. 04, 1992, pp. 665 679.

[15] S.D. Hanford, L.N. Long and J.F. Horn, A Small Semi-Autonomous Rotary-Wing Unmanned Air Vehicle (UAV), 2005. Available at: http://www.personal.psu.edu/lnl/papers/aiaa20057077.pdf

[16] G. Hoffmann, D. G. Rajnarayan, S. L. Waslander, D. Dostal, J. C. Jang and C. J. Tomlin, "The Stanford Testbed of Autonomous Rotorcraft for Multi-Agent Control (STAR-MAC)", *23rd Digital Avionics System Conference*, Salt Lake City, UT, November 2004.

[17] G. Hoffmann and S. L. Waslander, "Distributed Cooperative Search using Information-Theoretic Costs for Particle Filters, with Quadrotor Applications", *AIAA Guidance, Navigation, and Control Conference and Exhibit*, Keystone, Colorado, 21st-24th August 2006.

[18] H. Ichihashi, "Iterative fuzzy modelling and a hierarchical network". In: *Proc. 4th IFSA Congr., Brussels*, 1991, pp. 49-52.

[19] J.S.R. Jang, "ANFIS: adaptive-network-based fuzzy inference system", *IEEE Transactions System, Man and Cybernet*, vol. 23, issue 3, 1993, pp. 665-685.

[20] M. I. Jordan and D. Rumelhart, "Internal world models and supervised learning", *Proc. of the 8th Int. Workshop on Machine Learning*, 1991, pp. 70-74.

[21] H. Maaref, C. Barret, "Progressive optimization of a fuzzy inference system", *IFSA-NAFIPS'2001*, Vancouver, 2001, pp. 665-679.

[22] H. Maaref, C. Barret, "Sensor-based navigation of a mobile robot in an indoor environment", *Robotics and Autonomous Systems*, vol. 38, 2002, pp. 1-18.

[23] H. Maaref, K. M. Zemalache and L. Beji, "Self-Tunable Fuzzy Inference System: A comparative study for a drone", *International Fuzzy Systems Association (IFSA)*, Cancun, Mexico, 18th-21st June, 2007, pp. 691-700.

[24] L. Mederreg and F. Diaz and N. K. M'sirdi, "Nonlinear backstepping control with observer design for a 4 rotors helicopter", *AVCS'04, International Conference on Advances in Vehicle Control and Safety*, Genova, Italy, 28th-31st October, 2004.

[25] A. Mokhtari and A. Benallegue, "Dynamic feedback controller of Euler angles and wind parameters estimation for a quadrotor unmanned aerial vehicle". In: *Proceeding of the IEEE International Conference on Intelligent Robots and Systems*, April 2004, pp. 2359-2366.

[26] A. Mokhtari, A. Benallegue, B. Daachi, "Robustfeedback linearization and GH oo controller for a quadrotor unmanned aerial vehicle", *Journal of Electrical Engineering*, vol.57, no. 1, 2006, pp. 20-27.

[27] V. Mistler, A. Benallegue, N. K. M'Sirdi, "Exact Linearization and Noninteracting Control of a 4 Rotors Helicopter via Dynamic Feedback", *10th IEEE International Workshop on Robot-Human Interactive Communication*, 18th-21st September, 2001, Bordeaux and Paris.

[28] H. Nomura, I. Hayashi, N. Wakami, "A self-tuning method of fuzzy control by descent method", *Proc. 4thIFSA Congr.*, Brussels, 1991, pp. 155-158.

[29] P. Pound, R. Mahony, P. Hynes and J. Roberts, "Design of a four rotor aerial robot". In: *Proceeding of the Australasian Conference on Robotics and Automation*, Auckland, November 2002, pp. 145-150.

[30] T. Takagi and M. Sugeno, "Derivation of Fuzzy control rules from human operator 's control actions". In: *Proc. IFAC Symp. On Fuzzy Information, Knowledge Representation and Decision Analysis*, July 1983, pp. 55-60.

[31] A. Tayebi, S. McGilvray, "Attitude Stabilization of a VTOL Quadrotor Aircraft", *IEEE Transactions on Control Systems Technology*, vol. 14, no. 3, May 2006.

[32] G.P Tournier, M. Valenti, J.P How, "Estimation and Control of a Quadrotor Vehicle Using Monocular Vision and Moiré Patterns", *AIAA Guidance, Navigation,and Control Conference and Exhibit*, Keystone, Colorado, USA, AIAA2006-6711, 21st-24th August, 2006.

[33] L. X. Wang and J. M. Rendel, "Back-propagation fuzzy system as nonlinear dynamic system identifiers". In: *Proc. IEEE, Int. Conf. on fuzzy system*, San Diego, 1991,

pp. 1409-1416.

[34] S. L. Waslander, G. Hoffmann, J. S. Jang and C. J. Tomlin, "Multi-agent X4-flyer testbed control design: integral sliding mode vs. reinforcement learning", *IEEE/RSJ International Conference on Intelligent Robots and Systems*, 2005, pp. 468473.

[35] C. Yang, L. Lai and C. Wu, "Time-optimal control of a hovering quad-Rotor helicopter", *IEEE ICSS International Conference On Systems and Signals*, 2005, pp. 295-300.

[36] L. A. Young, E. W. Aiken, J. L. Johnson, R. Demblewski, J Andrews and J. Klem, "New concepts and perspectives on micro-rotorcraft and small autonomous rotary-wing vehicles". In: *Proceeding at the 20th AIAA Applied Aerodynamics Conference*, St. Louis, MO, USA, 2002.

[37] K. M. Zemalache, L. Beji and H. Maaref, "Two Inertial Models of X4-Flyers Dynamics, Motion Planning and Control", *Journal of the Integrated Computer-Aided Engineering (ICAE)*, vol. 14, no. 2, January 2007, pp. 107-119.

[38] K. M. Zemalache, L. Beji and H. Maaref, "Backstepping control technique: application to an under-actuated X4-flyer", *1st International in Computer System and Information Technology Conference*, Algeria, vol. 1, July 2005, pp. 151-156.

[39] K. M. Zemalache, L. Beji and H. Maaref, "Control of an under-actuated system: application to a four rotors rotorcraft". In: *5th IEEE International Conference on Robotics and Biomimetics*, Hong Kong, China, vol. 1, 29th June 3rd July, 2005, pp. 160-230.